Journal of Materials Chemistry C

Accepted Manuscript

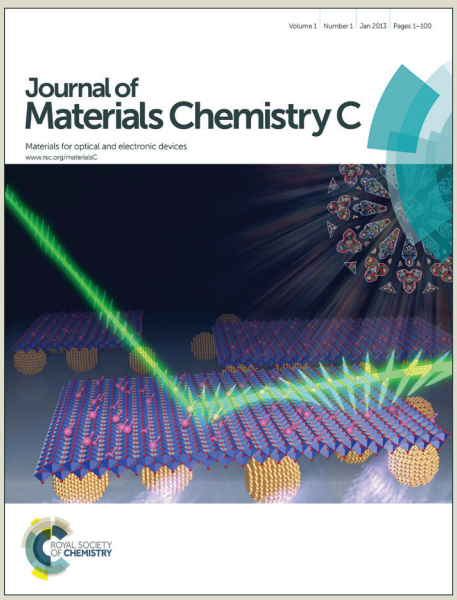

ROYAL SOCIETY OF CHEMISTRY

www.rsc.org/materialsC

Journal Materials Chemistry

Dynamic Article Links ►

Cite this: DOI: 10.1039/c0xx00000x

www.rsc.org/xxxxxx

Full papers

Low-Temperature Remote Plasma-Enhanced Atomic Layer Deposition of Graphene and Characterization of Its Atomic-Level Structure

Yijun Zhang, Wei Ren, Zhuangde Jiang, Shuming Yang, Weixuan Jing, Peng Shi, and Xiaoqing Wu, and Zuo-Guang Ye**

Journal Materials Chemistry

Dynamic Article Links ►

Cite this: DOI: 10.1039/c0xx00000x

www.rsc.org/xxxxxx

Full papers

Abstract:

Graphene has attracted a great deal of research interests owing to its unique properties and many potential applications. Chemical vapor deposition has shown some potential for the growth of large-scale and uniform graphene films, however, a high temperature (over 800 °C) is usually required for such growth. A whole new method for the synthesis of graphene at low temperatures by means of Remote Plasma-Enhanced Atomic Layer Deposition is developed in this work. Liquid benzene was used as a carbon source. Large graphene sheets with excellent quality were prepared at a growth temperature as low as 400 ^{o}C. The atomic structure of the graphene was characterized by means of aberration-corrected transmission electron microscopy. Hexagonal carbon rings and carbon atoms were observed, indicating a highly crystalline structure of the graphene. These results point to a new technique for the growth of high-quality graphene for potential device applications.

Journal Materials Chemistry

Dynamic Article Links ►

Cite this: DOI: 10.1039/c0xx00000x

www.rsc.org/xxxxxx

Full papers

Introduction

Graphene has attracted a great deal of interests because of its unique properties, such as remarkably high electron mobility (over 15,000 $cm^2V^{-1}s^{-1}$) at room temperature, high optical transparency and superior mechanical strength and flexibility,[1-11] which point to many potential applications in the next generation of electronic and optoelectronic devices. However, its development has been limited by the lack of viable techniques to produce uniform and large-scale graphene sheets. Until recently, the most popular technique had been mechanical exfoliation, which could only produce graphene of very small area with a low yield).[12] SiC sublimation could produce wafer-scale graphene sheets, but had some disadvantages such as high processing temperature and high cost of SiC substrate.[13] More recently, chemically assisted exfoliation of graphite was used to produce graphene which, unfortunately, contained many defects.[14] Chemical vapor deposition (CVD) has been widely employed to grow large size graphene.[15] However, current CVD route usually requires a high growth temperature, typically over 800 °C,[16-21] which greatly limits its application in graphene fabrication. Polymethylmethacrylate and other solid carbon sources were used to grow graphene on Cu foils by CVD.[22] A modified CVD route was employed to grow graphene on Cu foils at low temperatures, but the substrate needed to be annealed in H_2 at 1000 °C before growing graphene on it.[23] Therefore, low-temperature direct growth of graphene still remains a challenge.

Journal Materials Chemistry

Dynamic Article Links ►

Cite this: DOI: 10.1039/c0xx00000x

www.rsc.org/xxxxxx

Full papers

In this work, we have developed a new technique for the direct growth of graphene at low-temperature by means of remote Plasma-Enhanced Atomic Layer Deposition (PEALD) (A schematic of the remote PEALD is shown in Figure S1) which does not require a high temperature for the growth, nor a high temperature (typically over 1000 °C) to pre-anneal the Cu foil substrate before the deposition. Atomic layer deposition (ALD) is a unique deposition technique which is different from conventional film growth methods such as CVD. [24-26] Nowadays, ALD has become an important technique in the semiconductor industry since it can grow ultra-thin and conformal films. Unlike a CVD reaction, in which the precursors decomposes into the desired film and by-products at high temperatures (usually above the decomposition temperatures of the precursors), in ALD a very thin film is deposited layer by layer at a temperature much lower than the decomposition temperature of the precursor. There are four steps in a typical ALD major cycle: (1) pulse the first precursor into the reaction chamber, (2) purge the reaction chamber and remove the residual precursor and the by-products, (3) pulse the second precursor or another treatment to activate the surface again for the reaction, and (4) purge and evacuate the reaction chamber.

The remote plasma generator used in the experiment has a continuously turntable power from 100 W to 3000 W. It creates plasma in a separate chamber. The plasma is then transferred into the main reaction chamber, where the neutral radicals react on the surface of substrate. A major advantage of this process is to reduce ion-bombardment damage of the surface and thereby to

Journal Materials Chemistry

Dynamic Article Links ►

Cite this: DOI: 10.1039/c0xx00000x

www.rsc.org/xxxxxx

Full papers

improve the chemical reactivity of the reactants. The remote plasma provides a high plasma density with lower ion energy than other types of plasma, dramatically reducing the processing temperature.

The new method developed in this work based on the PEALD route uses Cu foils as substrate and a liquid carbon source. This method can grow graphene at a temperature much lower than reported previously, overcoming the disadvantage of high processing temperature required in CVD and related techniques. [16-20] Benzene is chosen as the carbon source because it contains the six-carbon-atomic-ring basic structural unit. The benzene molecules just need to be dehydrogenated and connect to each other to form the graphene structure, which further facilitates the growth process at low temperatures. Indeed, our results demonstrate that high-quality graphene sheets can be prepared on Cu foils at a temperature as low as 400 °C. The atomic level structure of the grown graphene has been analyzed by means of C_s-corrected high-resolution transmission electron microscopy (TEM). The Raman spectroscopy and electron energy-loss spectroscopy (EELS) have also been performed to characterize the graphene obtained.

Results and Discussion

For the deposition of grapheme by PEALD, we have performed a series of experiments and found that the growth by 10 ALD cycles is an optimum process that allows us to obtain monolayer graphene sheet with a large area. **Figure 1** gives the SEM images of a Cu foil pre-treated by acetic acid (A) and a graphene sheet grown on one of this type of substrates after an ALD process of 10

Journal Materials Chemistry

Dynamic Article Links ►

Cite this: DOI: 10.1039/c0xx00000x

www.rsc.org/xxxxxx

Full papers

cycles at 400 °C (B). **T**he Cu foil was pre-treated by acetic acid to remove the oxide layer on it and, as shown in Figure 1(A), its surface became relatively smooth compared with the un-treated one (see Figure S2 (A) in Supporting Information) although some surface striations (or stretcher strains) are still visible. It is worth noting that no pre-annealing of the Cu foils is needed in this process. **Figure 1**(B) shows that the graphene was uniformly grown on the Cu foil as the contrast of the graphene covering the Cu foil looks uniform across the area (A larger area SEM image is provided in Figure S2 (B), which confirms the uniformity of the graphene layer deposited). Note that an ALD deposition with less than 10 cycles will lead to a graphene sheet that is not homogenously monolayer and its area is small. On the other hand, a process with more than 10 cycles will result in a multilayered sheet and the number of layers increases with the increasing number of the ALD cycles. Additional TEM images of the graphene grown by 40 and 100 ALD cycles are shown in Figure S4 of Supporting Information, which reveal that 3- and 6-layered structures of the graphene grown by 40 and 100 ALD cycles, respectively. In summary, the monolayer graphene sheet grows larger with increasing ALD cycles and reaches its largest area at 10 ALD cycles. When the growth cycles are more than 10, multilayered graphene is formed with the number graphene layers increasing with the increased growth cycles.

The as-grown graphene was then transferred onto an ultra-thin amorphous carbon (α-*C*) film supported by a copper grid to be examined by means of transmission electron microscopy. Figure 2(A) shows the high-resolution TEM image of the graphene sheet and the α-*C* film. The boundary

Journal Materials Chemistry

Dynamic Article Links ►

Cite this: DOI: 10.1039/c0xx00000x

www.rsc.org/xxxxxx

Full papers

between the graphene and *α-C* films can be easily distinguished (see also in Figure S2 (C) of Supporting Information for a low-resolution TEM image which provides an overview of the large area and continuity of the grapheme layer). Representative areas of the graphene and the *α-C* film are marked by the yellow circles in Figure 2(A). Figure 2(B) gives the EELS spectra for the α-*C* area and the graphene area, respectively. The EELS spectra on the carbon *K*-edge are acquired by the Titan G2 high-resolution TEM from the same large region (marked by yellow circle in Fig. 2(A)) limited by the same aperture. The C *K*-edge at 284 eV on the EELS spectra (marked by the black line in Figure 2(B)) is characteristic of pure carbon, indicating the absence of contaminants in the graphene sample, such as N, and attesting to its high purity (N has an EELS spectrum with a visible edge starting at 393 eV, arising from the characteristic *K*-shell ionization edges of N, [27] and we were concerned that the carrying N_2 gas for benzene might enter the graphene as a dopant during the plasma period). The two spectra in Figure 2(B) might look similar. This is mainly because the α-carbon film is much thicker than the graphene sheet and, as a result, the background signal originated from the α-carbon film is so strong that it masks the sp^2 peak of the graphene and makes it look very weak. Nevertheless, a close inspection reveals that, despite the background noise of α-*C*, a weak π* peak appears at about 286 eV in the graphene spectrum, corresponding to the typical sp^2 coordinated carbon atoms in the graphene. [28] Moreover, the Raman spectrum (see Figure 4 below) also confirms the sp^2 hybridization in the grapheme. Therefore, it can be concluded

Journal Materials Chemistry

Dynamic Article Links ►

Cite this: DOI: 10.1039/c0xx00000x

www.rsc.org/xxxxxx

Full papers

from the EELS spectra in Figure 2 that pure graphene layer has been successfully grown by the PEALD technique.

The graphene layer number can be determined by analysis of the electron diffraction pattern. [23] Figure 3 shows the normal-incidence selected area electron diffraction pattern of the graphene grown by 10 ALD cycles, which was obtained by a JEOL 2100 TEM. It clearly exhibits a six-fold symmetry, as expected from graphene, [29-30] and the diffraction peaks can be indexed with the Miller–Bravais (*hkil*) indices. We may further differentiate the monolayer graphene from the multilayer graphene by inspecting the intensity ratio $I_{\{0\bar{1}10\}}/I_{\{\bar{2}110\}}$. Computational studies have shown that for multilayer graphene with the Bernal *AB* stacking, the intensity ratio $I_{\{0\bar{1}10\}}/I_{\{\bar{2}1100\}} < 1$, whereas, for monolayer graphene, $I_{\{0\bar{1}10\}}/I_{\{\bar{2}110\}} > 1$. [12] Figure 3 shows that the diffraction spots on the inner circle are obviously brighter than the outer circle spots, implying an intensity ratio $I_{\{0\bar{1}10\}}/I_{\{\bar{2}110\}} > 1$. This result indicates that the graphene layer deposited consists of a monolayer sheet.

Raman spectroscopy was performed to characterize the quality and thickness of the graphene. [31-33] Figure 4 shows the Raman spectrum of a graphene film transferred onto a 300 nm-thick SiO_2/Si substrate. Two sharp peaks are located at 1585 cm^{-1} and 2687 cm^{-1}, corresponding to the G and 2D bands, respectively. These two peaks have a symmetrical shape, which can be fitted by a single Lorentzian function. The graphene exhibits a large 2D/G ratio of ≈ 1.7, confirming that the probed film is a single-layer graphene sheet.[33] (Note that a weak disorder-induced D band was

Journal Materials Chemistry

Dynamic Article Links ►

Cite this: DOI: 10.1039/c0xx00000x

www.rsc.org/xxxxxx

Full papers

detected at 1350 cm^{-1}, which could arise from the presence of certain disordered structural defects induced by the transfer process or from the damage by the H_2 plasma.)

The atomic-resolution image of the graphene grown by 10 ALD cycles was obtained by means of the Titan G2 aberration-corrected high-resolution TEM. The white-atom contrast was achieved by using a negative value of spherical aberration in combination with a small positive defocus. [29] Figure 5 shows the high-resolution TEM image of the graphene obtained with an overfocus of about 5 nm and a spherical aberration of -11 μm. The carbon atoms in Figure 5 are shown in bright (an overview and more high-resolution TEM images of the graphene with different focus conditions can be found in Figure S2 (C) and Figure S3 of Supporting Information). The high-resolution TEM image in the red-framed area in Figure 5 is enlarged and filtered to display the atoms more clearly. As shown in Inset (A) of Figure 5, six-fold carbon rings are clearly observed, corresponding to the hexagonal structure of the graphene. These results indicate that the graphene grown by PEALD is of high structural quality (The TEM images and Raman spectra of the graphene grown by 40 and 100 ALD cycles can be found in Figure S4 of Supporting Information)

The distance between the second-nearest neighbour carbon atoms in the hexagonal carbon rings was measured using the Gatan's Digital-Micrograph software. Ten hexagonal lattice atomic distances were measured along the blue line in Inset (A) of Figure 5 to get an average value (and to reduce the measurement error). The intensity profile of the graphene along the blue line in Inset (A) is given in Inset B. It is known that the *C–C* bond length in graphite is 0.142 nm, [8] which implies

Journal Materials Chemistry

Dynamic Article Links ►

Cite this: DOI: 10.1039/c0xx00000x

www.rsc.org/xxxxxx

Full papers

that the distance between the second-nearest neighbour carbon atoms in the hexagonal carbon rings must be 0.2459 nm in an ideal graphene structure. Our measured value is 0.246 nm, which is in good agreement with the reported value for graphene and confirms that the graphene deposited is of high quality. [8]

Conclusions

A new technique has been developed to grow graphene sheets at low temperature from the liquid benzene carbon source by means of remote Plasma-Enhanced Atomic Layer Deposition (PEALD). This method features a much lower growth temperature than previously reported, overcoming the disadvantages of the conventional CVD method, such as high processing temperature and difficulties in controlling the number of graphene layers. The characterization of the morphology and atomic structure of the graphene by means of SEM, TEM and EELS shows that high-quality graphene sheets have been prepared on Cu foils at a temperature as low as 400 °C. The successful deposition of graphene by PEALD points to the possibility of integration of graphene into the semiconductor technologies in which the ALD technique has been widely used. Therefore, this work opens a new way to grow high-quality graphene for potential microelectronic device applications.

Experimental Procedure

Journal Materials Chemistry

Dynamic Article Links ►

Cite this: DOI: 10.1039/c0xx00000x

www.rsc.org/xxxxxx

Full papers

A remote plasma-enhanced ALD system (R200, Picosun) was employed to grow graphene. Liquid benzene (Alfa Aesar, 99.9%) and H_2/Ar_2 (99.9999%) mixture plasma were used as precursors. The benzene precursor gas from a stainless steel container was pulsed into the precursor line in the ALD pulse system and transported into the reaction chamber by N_2 carrying gas. The precursor was set to a temperature 5 °C lower than that in the delivery lines to prevent its condensation in the source lines. The remote plasma was generated by an inductively coupled plasma source operating in H_2/Ar_2 (at 60 sccm/60 sccm) with a total pressure of 60 Torr and a power of 3 kW or 2 kW at a frequency of 3.5 MHz. The substrate, a 25 μm-thick Cu foil (Alfa Aesar, 99.8%), was in turn ultrasonically cleaned using glacial acetic acid, acetone, absolute alcohol and deionized water for 10 minutes at a time. All the source lines were operated at a flow rate of 60 sccm N_2 or 60 sccm Ar and the reaction chamber pressure was kept at 10 Torr. When the temperature was stabilized at 400 °C, the Cu foil substrate was cleaned by H_2/Ar_2 plasma gas at 3 kW for 20 min. After the pretreatment, the following processing parameters were employed: the substrate temperature = 400 °C, the pressure = 10 Torr, and the time for each pulse cycle = 0.2 sec for benzene, 6 sec for N_2 purge, 9 sec for H_2/Ar_2 remote plasma and 3 sec for N_2 purge. A complete ALD cycle includes all the four steps mentioned above. An ALD process of 10 cycles was implemented in this work. After the deposition, the as-deposited film was cooled down to room temperature under a pure N_2 atmosphere.

Journal Materials Chemistry

Dynamic Article Links ►

Cite this: DOI: 10.1039/c0xx00000x

www.rsc.org/xxxxxx

Full papers

The morphology of the graphene is characterized by a scanning electron microscope (Qunta 250 FEG, FEI). Raman spectroscopy is carried out by a Raman spectrometer (Horiba Jobin Yvon R800, with a 514 nm excitation). The atomic structure and composition were investigated by means of an objective lens spherical aberration-corrected transmission electron microscope (FEI Titan G2 60-300) fitted with a Gatan Image Filter (GIF, Quantum 963). The Titan G2 high-resolution TEM was operated at 300 kV with an overfocus of about 5 nm, and the spherical aberration was tuned to -11 μm to achieve a negative spherical aberration (C_S) imaging (NCSI) condition. [34-36] The selected-area electron diffraction patterns of the graphene were obtained and examined by a conventional transmission electron microscope (JEOL 2100).

Supporting Information

Supporting Information is available from the RSC Online Library or from the authors.

Acknowledgments

This work is supported by the Natural Science Foundation of China (Grant Nos 90923001 and 51332003), the International Science & Technology Cooperation Program of China (Grant Nos. 2010DFB13640 and 2011DFA51880), the 'Changjiang Scholar Program' and the 'Qianren Program' of the Chinese Government, and the Natural Science and Engineering Research Council of Canada (NSERC). The authors thank C. S. Ma for help in TEM analysis.

Authors:

Journal Materials Chemistry

Dynamic Article Links ►

Cite this: DOI: 10.1039/c0xx00000x

www.rsc.org/xxxxxx

Full papers

Prof. W. Ren*

Electronic Materials Research Laboratory, Key Laboratory of the Ministry of Education & International Center for Dielectric Research, Xi'an Jiaotong University, Xi'an 710049, China.

Corresponding Author. E-mail: wren@mail.xjtu.edu.cn

Dr. Y. J. Zhang, Prof. P. Shi, Prof. X. Q. Wu

Electronic Materials Research Laboratory, Key Laboratory of the Ministry of Education & International Center for Dielectric Research, Xi'an Jiaotong University, Xi'an 710049, China.

Prof. Z. D. Jiang, Prof. S. M. Yang

State Key Laboratory for Manufacturing Systems Engineering, Xi'an Jiaotong University, Xi'an, 710049, China.

Prof. Z.-G. Ye*

Department of Chemistry and 4D LABS, Simon Fraser University, Burnaby, British Columbia, V5A 1S6, Canada and Electronic Materials Research Laboratory, Key Laboratory of the Ministry of Education & International Center for Dielectric Research, Xi'an Jiaotong University, Xi'an 710049, China

Corresponding Author. Email: zye@sfu.ca

Journal Materials Chemistry

Dynamic Article Links ►

Cite this: DOI: 10.1039/c0xx00000x

www.rsc.org/xxxxxx

Full papers

References:

[1] R. R. Nair, P. Blake, A. N. Grigorenko, K. S. Novoselov, T. J. Booth, T. Stauber, N. M. R. Peres, A. K. Geim, *Science* 2008, ***320***,1308.

[2] Ç. Ö. Girit, J. C. Meyer, R. Erni, M. D. Rossell, C. Kisielowski, L. Yang, C. H. Park, M. F. Crommie, M. L. Cohen, S. G. Louie, A. Zettl, *Science* 2009, ***323***, 1705.

[3] K. S. Novoselov, A. K. Geim, S. V. Morozov, D. Jiang, Y. Zhang, S. V. Dubonos, I. V. Grigorieva, A. A. Firsov, *Science* 2004, ***306***, 666.

[4] T. Ohta, A. Bostwick, T. Seyller, K. Horn, E. Rotenberg, *Science* 2006, ***313***, 951.

[5] J. S. Bunch, A. M. V. D. Zande, S. S. Verbridge, I. W. Frank, D. M. Tanenbaum, J. M. Parpia, H. G. Craighead, P. L. McEuen, *Science* 2007, ***315***, 490.

[6] K. Xu, P. G. Cao, J. R. Heath, *Science* 2010, ***329***, 1188.

[7] G. M. Rutter, J. N. Crain, N. P. Guisinger, T. Li, N. First, J. A. Stroscio, *Science* 2007, ***317***, 219.

[8] M. H. Gass, M. Gassi, U. Bangert, A. Bleloch, P. Wang, R. R. Nair, A.K. Geim, *Nature Nanotech.* 2008, ***3***, 676.

[9] M. H. Rümmeli, C. G. Rocha, F. Ortmann, I. Ibrahim, H. Sevincli, F. Börrnert, J. Kunstmann, A. Bachmatiuk, M. Pötsche, M. Shiraishi, M. Meyyappan, B. Büchner, S. Roche, G. Cuniberti, *Adv. Mater.* 2011, ***23***, 4471.

Journal Materials Chemistry

Dynamic Article Links ►

Cite this: DOI: 10.1039/c0xx00000x

www.rsc.org/xxxxxx

Full papers

[10] C. G. Lee, X. D. Wei, J. W. Kysar, J. Hone, *Science* 2008, ***321***, 385.

[11] A. K. Geim, K. S. Novoselov, *Nature Mater*. 2007, ***6***, 83.

[12] Y. Hernandez, V. Nicolosi, M. Lotya, F. M. Blighe, Z.Y. Sun, S. De, I. T. McGovern, B. Holland, M. Byrne, Y. K. Gun'Ko, J. J. Boland, P. Niraj, G. Duesberg, S. Krishnamurthy, R. Goodhue, J. Hutchison, V. Scardaci, A. C. Ferrari, J. N. Coleman, *Nature Nanotech.* 2008, ***3***, 563.

[13] A. K. Geim, *Science* 2009, ***324***, 1530.

[14] G. N. Cristina, J. C. Meyer, R. S. Sundaram, A. Chuvilin, S. Kurasch, M. Burghard, K. Kern, U. Kaiser, *Nano Lett.* 2010, ***10***, 1144.

[15] A. Reina, X. T. Jia, J. Ho, D. Nezich, H. Son, V. Bulovic, M. S. Dresselhaus, J. Kong, *Nano Lett.* 2009, ***9***, 30.

[16] X. S. Li, **W. W.** Cai, J. An, S. Kim, J. Nah, D. Yang, R. Piner, A. Velamakanni, I. Jung, E. Tutuc, S. K. Banerjee, L. Colombo, R. S. Ruoff, *Science* 2009, ***324***, 1312.

[17] S. Bae, H. Kim, Y. Lee, X. F. Xu, J. S. Park, Y. Zheng, J. Balakrishnan, T. Lei, H. R. Kim, Y. II. Song, Y. J. Kim, K. S. Kim, B. Özyilmaz, J. H. Ahn, H. B. Hong, S. Iijima, *Nature Nanotech*. 2010, ***5***, 574.

[18] S. Lee, K. Lee, Z. H. Zhong, *Nano Lett*. 2010, ***10***, 4702.

[19] X. S. Li, W. W. Cai, L. Colombo, R. S. Ruoff, *Nano Lett*. 2009, ***9***, 4268.

Journal Materials Chemistry

Dynamic Article Links ►

Cite this: DOI: 10.1039/c0xx00000x

www.rsc.org/xxxxxx

Full papers

[20] X. S. Li, C. W. Magnuson, A. Venugopal, J. An, J. W. Suk, B. Y. Han, M. Borysiak, W. W. Cai, A. Velamakanni, Y. W. Zhu, L. F. Fu, E. M. Vogel, E. Voelkl, L. Colombo, R. S. Ruoff, *Nano Lett*. **2010**, *10*, 4328.

[21] S. Bhaviripudi, X. Jia, M. S. Dresselhaus, J. Kong, *Nano Lett*. **2010**, *10*, 4128.

[22] Z. Z. Sun, Z. Yan, J. Yao, E. Beitler, Y. Zhu, J. M. Tour, *Nature* **2010**, *468*, 549.

[23] Z. C. Li, P. Wu, C. X. Wang, X. D. Fan, W. H. Zhang, X. F. Zhai, C. G. Zeng, Z. Y. Li, J. L. Yang, J. G. Hou, *Nano Lett*. **2011,** *5*, 3385.

[24] S. M. George, *Chem. Rev.* **2010**, *110*, 111.

[25] T. Suntola, *Thin Solid Films* **1992**, *216*, 84.

[26] R. L. Puurunen, J. Saarilahtia, H. Kattelusa, *ECS Trans*, **2007**, *11*, 3.

[27] L. J. Ci, L. Song, C. H. Jin, D. Jariwala, D. X. Wu, Y. J. Li, A. Srivastava, Z. F. Wang, K.Storr, L. Balicas, F. Liu, P. M. Ajayan, *Nature Mater.* **2010**, *9*, 430.

[28] K. Suenaga, M. Koshino, *Nature* **2010**, *468*, 1088.

[29] C. L. Jia, M. Lentzen, K. Urban, *Science* **2003**, *299*, 870.

[30] J. C. Meyer, A. K. Geim, M. I. Katsnelson, K. S. Novoselov, D. Obergfell, S. Roth, C. Girit, A. Zettl, *Solid State Comm*. **2007**, *143*, 101.

[31] J. C. Meyer, A. K. Geim, M. I. Katsnelson, K. S. Novoselov, T. J. Booth, S. Roth, *Nature* **2007**, *446*, 60.

[32] A. Gupta, G. Chen, P. Joshi, S. Tadigadapa, *Nano Lett.* **2006**,*6*, 2667.

Journal Materials Chemistry

Dynamic Article Links ►

Cite this: DOI: 10.1039/c0xx00000x

www.rsc.org/xxxxxx

Full papers

[33] Y. Ogawa, B. S. Hu, C. M. Orofeo, M. Tsuji, K. I. Ikeda, S. Mizuno, H. Hibino, H. Ago, *J. Phys. Chem. Lett.* **2012**, *3*, 219.

[34] J. C. Meyer, C. Kisielowski, R. Erni, M. D. Rossell, M. F. Crommie, A. Zettl, *Nano Lett*. **2008**, *8*, 3582.

[35] H. Kim, H. B. R. Lee, W. J. Maeng, *Thin Solid Films* **2009**, *517*, 2563.

[36] C. L. Jia, M. Lentzen, K. Urban, *Microsc. Microanal*. 2004, *10*, 174.

Journal Materials Chemistry

Dynamic Article Links ►

Cite this: DOI: 10.1039/c0xx00000x

www.rsc.org/xxxxxx

Full papers

Figure Captions

Figure 1 SEM images of a Cu foil pre-treated by acetic acid (A) and the graphene sheet grown on one of this kind of substracts by 10 ALD cycles at 400 °C (B).

Figure 2 (A) High-resolution TEM image of the amorphous *C* (α-*C*) film and the graphene on it (by the Titan G2 TEM). (B) EELS spectra of carbon *K*-edge obtained from the α-C film area and the graphene area (on the α-*C* film) marked by yellow circles in (**A**) (the spectra were recorded under the same electron-optical conditions).

Figure 3 Normal-incidence selected area electron diffraction pattern of the graphene grown by 10 ALD cycles (by the JEOL 2100 TEM).

Figure 4 Raman spectrum of the graphene grown by 10 ALD cycles and transferred on a 300 nm-thick SiO_2/Si substrate, with an excitation wavelength of λ= 514 nm. Insets are the schematic diagrams of E_{2g} and A_{1g} stretching modes, corresponding to the G and D peaks, respectively

Journal Materials Chemistry

Dynamic Article Links ►

Cite this: DOI: 10.1039/c0xx00000x

www.rsc.org/xxxxxx

Full papers

Figure 5 High-resolution images of the graphene deposited by 10 ALD cycles. The atomic-resolution image was obtained using FEI Titan G2 60-300 at an acceleration voltage of 300 kV (the scale bar is 2 nm). Inset (**A**): Filtered image of the area within the red rectangular frame. Inset (**B)**: Pixel intensity profile of the graphene along the blue line in Inset (**A)**, which was used to calculate the distance between the second-nearest neighboring carbon atoms in the hexagonal carbon rings using the Digital Micrograph software.

Journal Materials Chemistry

Dynamic Article Links ►

Cite this: DOI: 10.1039/c0xx00000x

www.rsc.org/xxxxxx

Full papers

Figure 1 (A-B)

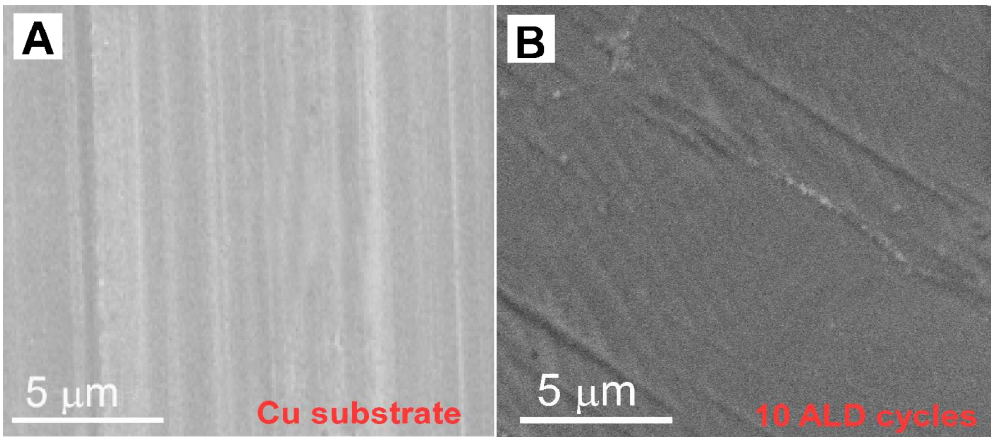

Journal Materials Chemistry

Dynamic Article Links ►

Cite this: DOI: 10.1039/c0xx00000x

www.rsc.org/xxxxxx

Full papers

Figure 2(A-B)

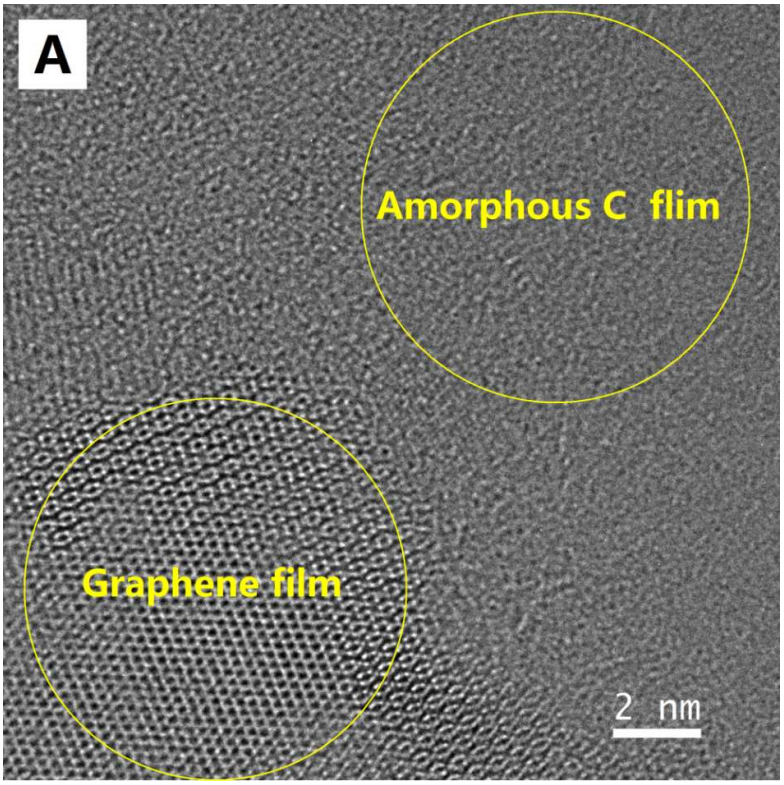

Journal Materials Chemistry

Dynamic Article Links ►

Cite this: DOI: 10.1039/c0xx00000x

www.rsc.org/xxxxxx

Full papers

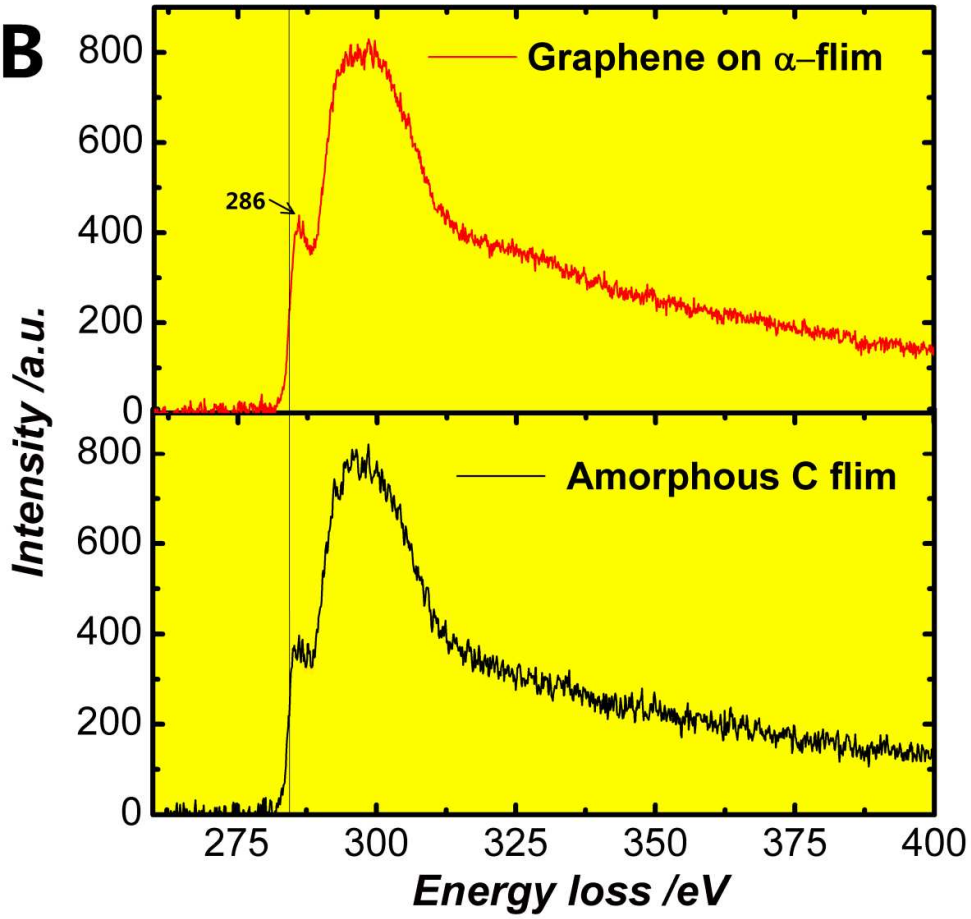

Journal Materials Chemistry

Dynamic Article Links ►

Cite this: DOI: 10.1039/c0xx00000x

www.rsc.org/xxxxxx

Full papers

Figure 3

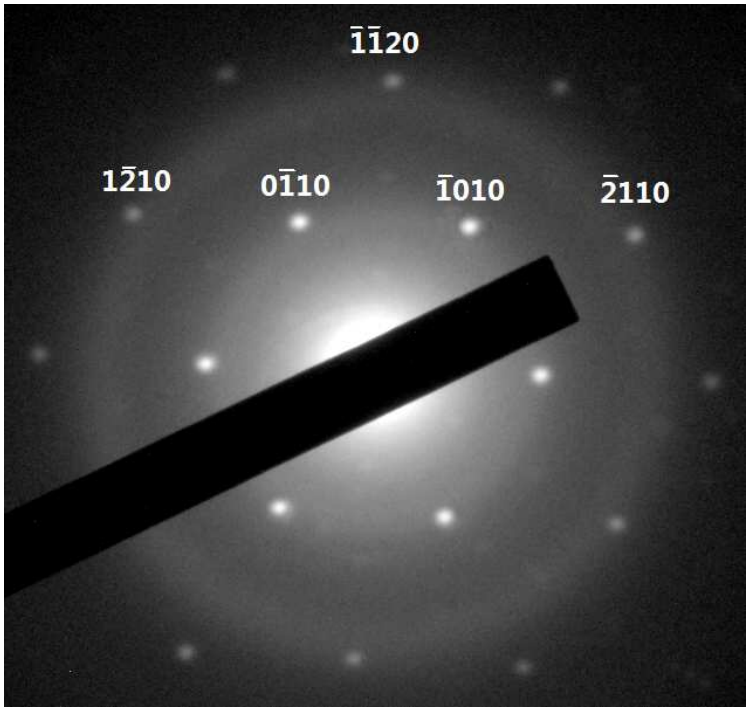

Journal Materials Chemistry

Dynamic Article Links ►

Cite this: DOI: 10.1039/c0xx00000x

www.rsc.org/xxxxxx

Full papers

Figure 4

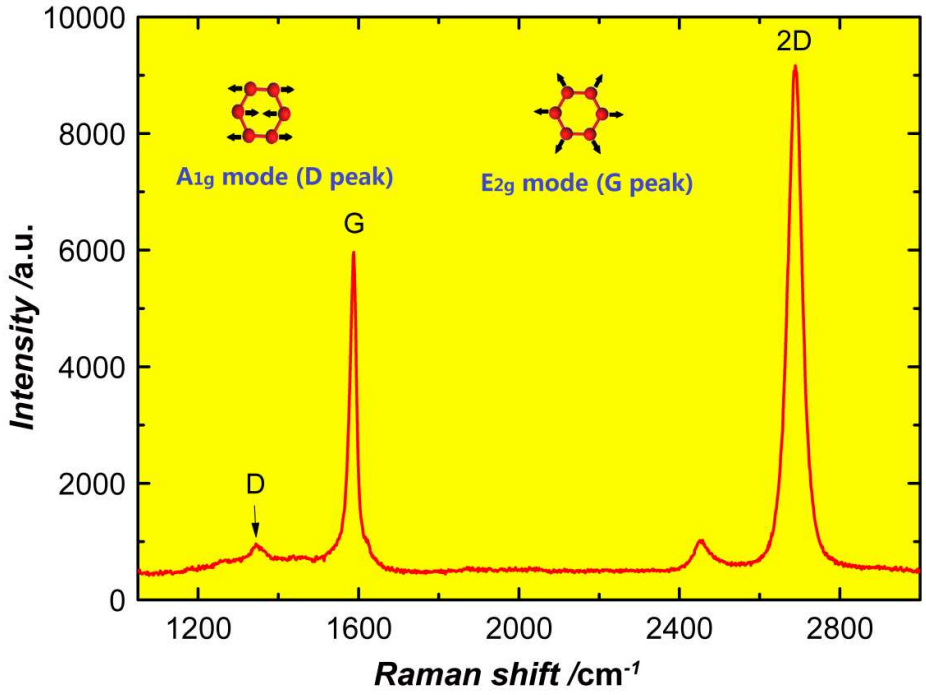

Journal Materials Chemistry

Dynamic Article Links ►

Cite this: DOI: 10.1039/c0xx00000x

www.rsc.org/xxxxxx

Full papers

Figure 5

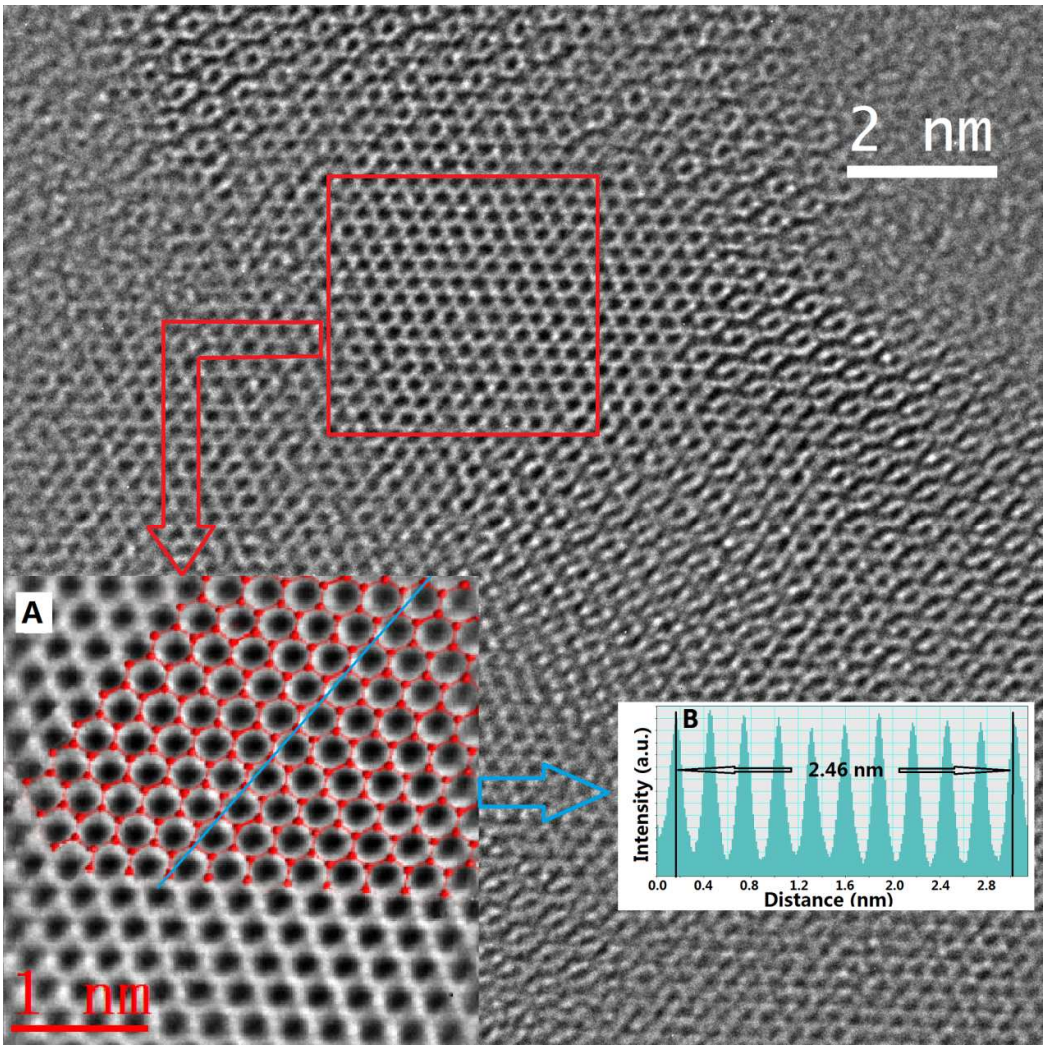

Atomic-Resolution Image of Graphene Sheet Synthesized by Remote Plasma-Enhanced Atomic Layer Deposition at Low Temperatures.